Validation and Sub-grid Scale Characteristics of an Upwind, Five-Equation, Two-Phase Model for Cavitating Flows

Sophie A. Wood[1] and Daniel V. Foti[2]
University of Memphis, Memphis, TN, 38152, United States of America

Numerical dissipation and accuracy in large-eddy simulations for cavitating flows are often negatively affected by flow discontinuities such as shock waves generated by vapor-bubble collapse, vapor-liquid phase boundaries, and complexities of solid boundaries, especially if the flow is under-resolved. An expedient solution is to leverage the numerical discretization error of monotone, sharp-interface capturing schemes to mimic the physical dissipation rate. This methodology eschews traditional explicit sub-grid scale models and is referred to as implicit large-eddy simulation. A specific upwind Godunov-based scheme using an HLLC Reimann solver and five-equation two-phase flow numerical model for cavitating flows is constructed and discretized in generalized curvilinear coordinates. Because the variable reconstruction is performed locally, the scheme can capture both discontinuities and low Mach number features. The scheme is characterized in the following: (1) Modified equation analysis is employed to theoretically derive the dissipation behaviors and (2) Simulations of a two-phase shock tube and the Taylor-Green vortex are undertaken for validation and numerical experimentation. The shock tube profiles of velocity, total energy, and void fraction are in good agreement with experiments.

I. Introduction

The motivation for these simulations concerns cavitation and cavitation erosion. Cavitation erosion is a prevalent issue today because of the costly damage it causes to surfaces such as ships, propellers, and rudders. This damage is significant and must be mitigated. A prime example of this issue lies within the United States Navy. They recently had to redesign a rudder on an entire class of ships, the *USS Arleigh Burke*, due to damage caused by cavitation erosion[1]. The paint and material on the rudder are clearly eroded away due to the repeated impingement of cavities on the surface. Another issue concerning cavitation is that cavitation causes propellers to have a lower performance, due to energy being lost to phase change during cavitation. Cavitation is also a noisy process, which makes ships more detectable and harder to be stealthy, which is not favorable in the context of military applications. Another important motivation for simulating cavitation is its use in the medical field. Cavitation is used to remove kidney stones in a non-invasive medical procedure. Our fundamental problem is that cavitation erosion is a costly damage mechanism, and simulating cavitation could resolve, or at least mitigate, this issue.

Before we investigate cavitation erosion, we must efficiently capture cavitation processes at the industrial scale with large Reynolds numbers, and impose arbitrary complex boundaries. Cavitation erosion experiments at the industry level are not only very difficult to perform, they are also very expensive and, for the most part, infeasible. Simulations of cavitation erosion are also costly. There have been numerous investigations of cavitation employing large-eddy simulations with explicit sub-grid scale models, including incompressible (Eulerian-Lagrangian) approaches[2] and compressible approaches[3].

Turbulent flows and cavitation are difficult to solve experimentally and are also difficult to observe, and lab experiments with cavitation erosion do not scale well. Simulations can bridge this gap, but do have some problems.

[1] Undergraduate Student, Department of Mechanical Engineering, AIAA Student Member
[2] Assistant Professor, Department of Mechanical Engineering, AIAA Faculty Member

They can be difficult and infeasible to solve at large Reynolds numbers, and the small-scale eddies cannot be disregarded. There needs to be a pathway to dissipate these small-scale eddies effectively. In large-eddy simulations, the large-scale eddies are directly computed, while the small-scale eddies are modeled. Small-scale eddies can be modeled because they are isotropic, meaning that they are often similar any way you look at them and are universal. These small-scales can be modeled in different ways: functional, structural, or implicit. In a functional model, a function is directly used to represent their behavior, while in structural or implicit, a structure is created to model this behavior.

In implicit large-eddy simulations (iLES), there is no explicit sub-grid scale used. Even though this method has been around for a while, it has been largely disregarded. This method was first proposed by Ref. 6 in 1992, called monotone integrated LES. The idea behind iLES is that it has been observed that specific dissipative schemes mimic physical dissipation. This means that large scales can be captured, while small dissipative scales can be modeled based on numerical dissipation in high Reynolds number flows[4,5,7-10]. A class of iLES is based on monotonic upwind finite volume methods. A scheme must have dissipation in order to have a stable partial differential equation and to be solved computationally.

There have been relatively few studies of turbulence cavitating flow simulations that employ implicit large-eddy simulations. Examples of those who employed implicit large-eddy simulations are an incompressible iLES solver for a cavitating propeller, and compressible iLES using Adaptive Local Deconvolution Method.[2,3] There has been very little rigorous investigation into how monotonic upwind finite volume schemes behave in two-phase, cavitating flows. The purpose of this work is to investigate how an effective two-phase flow solver with iLES can be employed to solve high Re flows. We will validate a two-phase flow model that has numerical properties similar to compressible solvers used for iLES and develop the theoretical background of numerical dissipation using modified equation analysis.

II. Methodology and Numerical Methods

The approach is based on the five-equation model which models a single pressure and energy between the two phases of the fluid[15]. The models are a compressible two-phase system, which allows us to capture the physics of phase change, mass transfer, and shocks. The original five-equation model is not conservation form because of the equation governing the transport of the volume fraction. However, to employ conventional shock capturing finite volume schemes, the equations need to be in conservative form. Following Ref. 16, the equations for the conservation phasic mass, momentum, energy, and volume fraction are given by the following equations:

$$\frac{\partial \alpha_1 \rho_1}{\partial t} + \frac{\partial}{\partial x_i}(\alpha_1 \rho_1 u_i) = 0$$

$$\frac{\partial \alpha_2 \rho_2}{\partial t} + \frac{\partial}{\partial x_i}(\alpha_2 \rho_2 u_i) = 0,$$

$$\frac{\partial \rho u_i}{\partial t} + \frac{\partial}{\partial x_j}\left(\rho u_i u_j + p\right) = 0,$$

$$\frac{\partial \rho E}{\partial t} + \frac{\partial}{\partial x_i}[u_i(\rho E + p)] = 0,$$

$$\frac{\partial \alpha_1}{\partial t} + \frac{\partial u_i \alpha_1}{\partial x_i} = H(\alpha_1, \rho_1, \rho_2, p)\frac{\partial u_i}{\partial x_i},$$

where α_i is the volume fraction subject to the condition $\alpha_1 + \alpha_2 = 1$, ρ_i is the phasic density, u_i is the velocity in three directions, E is the total energy, p is the pressure, and H is given by

$$H = \frac{\alpha_1 \rho_2 c_2^2}{\alpha_2 \rho_1 c_1^2 + \alpha_1 \rho_2 c_2^2},$$

where c_i is the phasic speed of sound. The conversion of the volume fraction transport equation into conservation form was shown to not have a large impact on the flow in Ref. 16. The five-equation model has 5 equations and 6 unknowns and requires a stiffened equation of state to account for the two phases. Because this is a two-phase model, it is much more difficult to solve than an ideal gas. The stiffened equation of state for each phase is given by the following:

$$p_k(e_k, \rho_k) = (\gamma_k - 1)\rho_k e_k - \gamma_k p_k^{\infty} - (\gamma_k - 1)\rho_k q_k,$$

where γ_k, p_k^{∞}, and q_k are calibrated parameters, and e_k is the internal energy of the kth phase. All parameters are obtained from calibration of specific materials. This five-equation model involves fractional, two step method defined by Saurel (2009): (1) integration of the conservation equations, and (2) imposition of heat and mass transfer by updating the thermodynamic variables by imposing thermodynamic equilibrium on the system. The thermodynamic variables are updated using a relaxation scheme by Ref. 14.

Numerical methods

The five conservation equations are integrated in a three-dimensional finite volume scheme for the flux *F* with the following equation based on a similar scheme of the single-phase Euler equations[5]:

$$\frac{\{\partial U\}}{\partial t} + \frac{\{\partial F\}}{\partial x} = 0,$$

where

$U = [\alpha_1\rho_1, \alpha_2\rho_2, \rho u, \rho v, \rho w, \rho E, \alpha_1]^T,$

$F = [\alpha_1\rho_{1u}, \alpha_2\rho_2 u, \rho u^2, \rho uv, \rho uw, \rho uE, \alpha_1 u]^T.$

The fluxes are solved using the HLLC Riemann[11] solver at the cell interfaces. Higher order accurate using MUSCL extrapolation[12],

$P^L_{i+\frac{1}{2}} = P_i + \frac{1}{2}\phi^{lim}(r^L)(P_i - P_{i-1})$ and $P^R_{i+\frac{1}{2}} = P_{i+1} + \frac{1}{2}\phi^{lim}(r^R)(P_{i+2} - P_{i+1}),$

where *P* is the vector of cell averaged primitive variables and r is given by

$r^L = \frac{P_{i+1}-P_i}{P_i-P_{i-1}}$ and $r^R = \frac{P_i-P_{i-1}}{P_{i+1}-P_i}$.

A fifth order reconstruction[13] with a diffusive limiter ϕ^{lim}used. The limiter first computes

$\Phi_L = \frac{-\frac{2}{r_{i-1}^{lim,L}} + 11 + 24r_i^{lim,L} - 3r_i^{lim,L}r_{i+1}^{lim,L}}{30}$ and $\Phi_R = \frac{-\frac{2}{r_{i+1}^{lim,R}} + 11 + 24r_{i+1}^{lim,R} - 3r_{i+1}^{lim,R}r_i^{lim,R}}{30},$

Monotonicity is maintained with the following:

$\phi_L^{lim} = \max\left(0, \min\left(2, 2r_i^{lim,L}, \Phi_L\right)\right)$ and $\phi_R^{lim} = \max\left(0, \min\left(2, 2r_i^{lim,R}, \Phi_R\right)\right).$

The time integration uses a third order strong stability preserving Runge-Kutta scheme for an overall fifth order in space and third order in time scheme. The time integration is given in the following three steps:

$$U_i^1 = U_i^n + \frac{1}{2}\frac{\Delta t}{\Delta x} f(U_i^n),$$

$$U_i^2 = U_i^n + \frac{1}{2}\frac{\Delta t}{\Delta x} f(U_i^1),$$

$$U_i^{n+1} = \frac{1}{3}\left(2U_i^2 + U_i^n + \frac{\Delta t}{\Delta x}[f(U_i^2) + f(U_i^1)]\right),$$

where $f(U_i)$ is the flux function derived above. This has a stability region to a theoretical limit of CFL = 2.

III. Results

We present several test cases for validation of the numerical methods. First, we begin with validation of the scheme with two shock tube problems in two-phase fluids. In the first case, we do not activate the thermo-chemical relaxation,

while in the second case, the effects of the relaxation are applied. We then provide theoretical analysis of the modified equation analysis and introduce the Taylor-Green vortex.

A. Dodecane Liquid-Vapor Shock Tube

The shock tube problem from Ref. 14. contains liquid dodecane at a high pressure $p_l = 10^8$ Pa with density $\rho_l = 500$ kg m^{-3} on the left side of the tube. On the right side of the tube vapor dodecane is at atmospheric pressure with a density $\rho_v = 2$ kg m^{-3}. The shock tube is 1 m long and the interface between the liquid and vapor is placed at 0.75 m. For numerical stability, a weak volume fraction of 10^{-8} of the other phase is enforced at initiation. The problem is solved as a contact discontinuity as the heat and mass transfer for not included. The shock tube is simulated for t = 473 μs. A relatively low resolution of 1000 points is used compared to results in Ref. 15. Figure 1 shows the conventional three waves that form during the propagation of the shock. A left facing rarefaction wave moves through the liquid on the left, there is a contact discontinuity between the two phases, and a shock propagating through the vapor. The results in Fig. 1 shows that the propagation of the waves can be captured and is reasonably well agreement given the resolution of the grid.

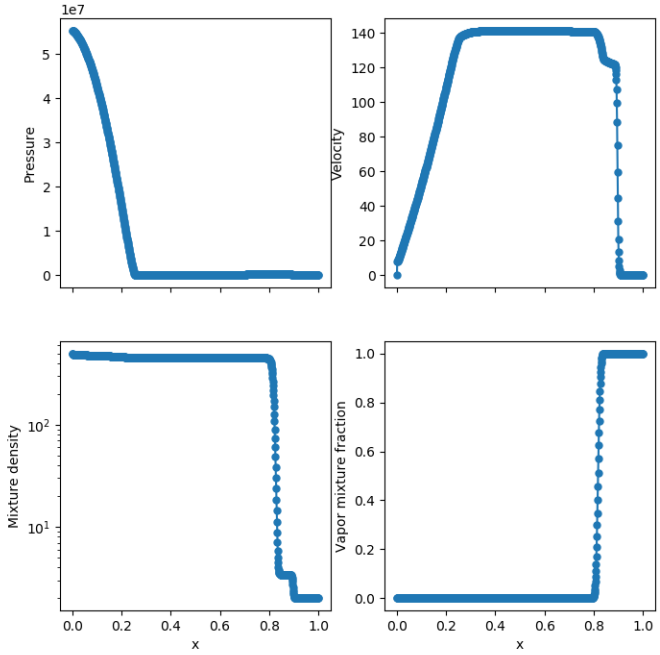

Figure 1: Dodecane liquid–vapor shock tube without mass transfer.

B. Water Cavitation Tube

The validation used for this scheme is a water cavitation tube problem with water-liquid vapor expansion in one dimension in a 1 m tube[14,15]. The tube is filled with liquid water with density $\rho_l = 1150$ kg m^{-3} at atmospheric pressure. A uniform distribution of vapor at $\alpha_v = 10^{-2}$ is placed in the domain. The velocity is set to be u = |2| m/s where the left side of the tube is u = -2 m/s and the right side of the tube is at 2 m/s where the interface is at x = 0.5 m. The flow in opposite directions forces a low pressure at the center. The pressure drops below critical vapor pressure for cavitation to occur, causing vapor to form. In this problem, we choose two different tests for heat and mass transfer. For the first test pT relaxation, there is not mass transfer between the phases. Figure 2 shows the results for the test. Because there is no mass transfer between phases, the pressure of the pT relaxation case can

continue to decrease at the center, but no water vapor is formed. A second case pT-pTg, which accounts for mass transfer between the two phases shows a marked increase in water vapor in terms of volume and mass fraction at the center of the tube in Figure 2. The results for both cases are in good agreement with the results in Ref. 14 despite using 1000 grid points compared to 5000 by Ref. 14.

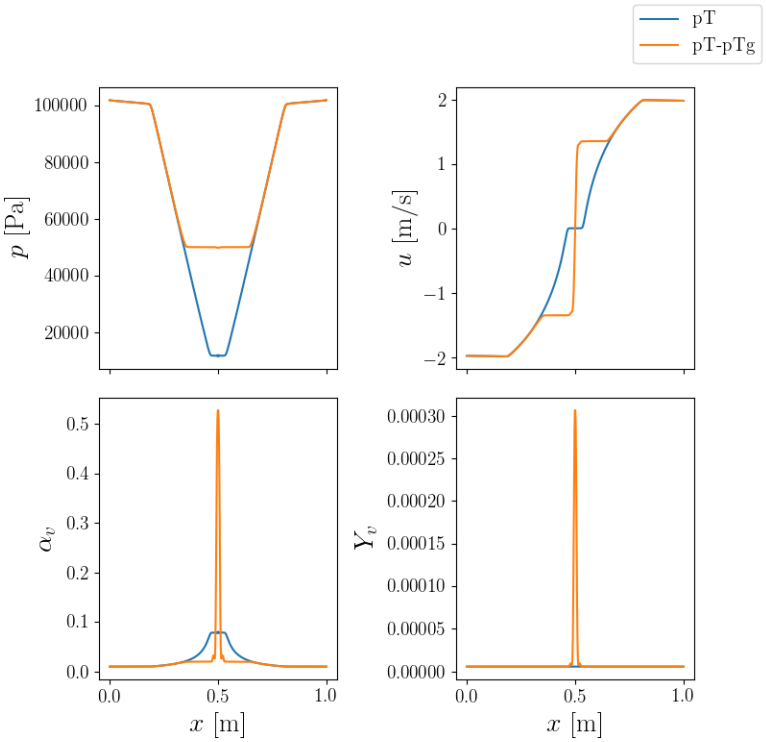

Figure 2: Numerical results for the water cavitation tube test with initial velocity |u| =2 m/s at time t = 3.2 ms.

C. Modified Equation Analysis

Schemes that are employed for iLES often come from a certain class of schemes where the unresolved scales can be represented by the truncation error of the discretization. However, the numerical dissipation caused by the truncation error must be carefully examined for iLES when considering high Reynolds number flows. Modified equation analysis uses a nonlinear Taylor series expansion. Modified equation analysis allows us to quantify diffusive and dispersive terms that will affect the solution to compare to what is desired, physical dissipation[4,5]. The procedure begins with

expanding the state variable in a Taylor series and the equation is reorganized to equate to the time derivative as following:

$$\frac{U_i^{n+1} - U_i^n}{\Delta t} = \frac{\partial U}{\partial t} + \frac{\Delta t}{2}\frac{\partial^2 U_i}{\partial t^2} + \frac{\Delta t^2}{6}\frac{\partial^3 U_i}{\partial t^3} + O(\Delta t^4).$$

The expansion of the state variables is substituted into the governing equations including into the fluxes. Using the governing equations, the time derivatives are substituted for spatial derivatives. Finally, the accumulation of all terms from expansion can be written as following:

$$\frac{\partial U_i}{\partial t} + \frac{\partial F_i}{\partial x} = R_{ij} + O(\Delta t^3, \Delta x^3),$$

where R_{ij} contains all spatial and temporal derivatives term from the expansion. Because these terms are the result of discretization and truncation, they represent additional terms that are numerical solved. In the context of iLES, the sub-grid scale (SGS) stress is related to these terms as following:

$$R_{ij}^{SGS} = R_{ij} + O(\Delta t^3, \Delta x^3).$$

The leading even terms due to the scheme and limiting are related to the numerical dissipation. For the scheme, the numerical dissipation is the same as the kinetic energy dissipation, ϵ, where the leading terms are

$$\epsilon = \frac{\Delta x^3}{60} z a u_x u_{xxxx} \sim \frac{|u|^3}{\Delta x}.$$

Through using modified equation analysis, implicit sub-grid scales and numerical dissipation can effectively be modeled. The last equation shown above is the numerical dissipation of the scheme, which compares closely to Kolmogorov's four-fifths law[5]. This indicates the chosen scheme can theoretically be employed for implicit LES.

D. Taylor-Green Vortex Case

The Taylor Green vortex is a canonical turbulence test case with large scale structures, vortex breakdown, a maximum dissipation limit, and decaying turbulence. The large structures initial shown in Fig. 3 continuously break each other apart. A turbulent flow initiates with broad scales as shown in Fig. 4. As part of future work, the scheme will be tested at several resolutions to test the theoretical results of the modified equation analysis.

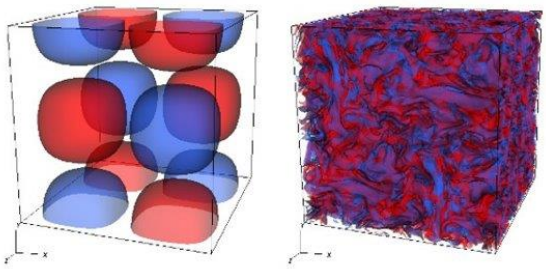

Figure 3. Taylor-Green Vortex Case

IV. Conclusion

The five-equation model provides an efficient and effective method to capture cavitation and shock waves of two-phase flow. It is especially adept at capturing the interface between phases. The model is built in a high-order finite volume scheme that is total variation diminishing and preserves monotonicity. Two test case of shock tubes were undertaken to validate the scheme and assess heat and mass transfer. The thermo-chemical relaxation can account of the mass transfer between the phases. The particular interest in this scheme is the function of its truncation terms from numerical discretization. Using modified equation analysis, the kinetic energy dissipation is shown to be similar to Kolmogorov's four-fifths law. This is important for high Re number flows where it is infeasible perform direct numerical simulation and capture all length scales. The scheme can theoretically ensure that the turbulent dissipation is match by the truncation error and always the scheme to forgo any explicit turbulence modeling. The Taylor-Green

vortex case is setup to test the dissipation. In the future, we will assess dissipation with the Taylor-Green vortex and other canonical turbulent flows. We will continue to identify implicit sub-grid scale characteristics in turbulent and cavitating flows.

References

[1] "Effects of Ship Hull and Propeller on Rudder Cavitation." Shen, et al. J. Ship Res. 1997

[2] Asnaghi, Abolfazl, Andreas Feymark, and Rickard E. Bensow. "Computational analysis of cavitating marine propeller performance using OpenFOAM." *Proceedings of the Fourth International Symposium on Marine Propulsors (smp'15), Austin, TX, USA*. Vol. 31. 2015.

[3] Egerer, Christian. Large-Eddy Simulation of Turbulent Cavitating Flows. Diss. Technische Universität München, 2016.

[4] Foti, Daniel, and Karthik Duraisamy. "Subgrid-scale characterization and asymptotic behavior of multidimensional upwind schemes for the vorticity transport equations." *Physical Review Fluids* 6.2 (2021): 024606.

[5] Thornber, Ben, et al. "An improved reconstruction method for compressible flows with low Mach number features." *Journal of Computational Physics* 227.10 (2008): 4873-4894.

[6] JP Boris, FF Grinstein, ES Oran, and RL Kolbe, "New insights into large eddy simulation," *Fluid Dynamics Research* 10, 199–228 (1992).

[7] Len G Margolin and William J Rider, "A rationale for implicit turbulence modelling," *International Journal for Numerical Methods in Fluids* 39, 821–841 (2002).

[8] LG Margolin and WJ Rider, "The design and construction of implicit LES models," *International Journal for Numerical Methods in Fluids* 47, 1173–1179 (2005).

[9] LG Margolin, WJ Rider, and FF Grinstein, "Modeling turbulent flow with implicit LES," *Journal of Turbulence*, N15 (2006).

[10] Dimitris Drikakis, Marco Hahn, Andrew Mosedale, and Ben Thornber, "Large eddy simulation using high-resolution and high-order methods," *Philosophical Transactions of the Royal Society A: Mathematical, Physical and Engineering Sciences* 367, 2985–2997 (2009).

[11] Toro, Eleuterio F. "The Equations of Fluid Dynamics." *Riemann Solvers and Numerical Methods for Fluid Dynamics: A Practical Introduction* (1997): 1-39.

[12] B. van Leer. "Towards the ultimate conservative difference scheme.IV. A new approach to numerical convection." *Journal of Computational Physics* 23 (1977) 276–299.

[13] Kim, Kyu Hong, and Chongam Kim. "Accurate, efficient and monotonic numerical methods for multi-dimensional compressible flows: Part II: Multi-dimensional limiting process." *Journal of Computational Physics* 208.2 (2005): 570-615.

[14] Pelanti, Marica, and Keh-Ming Shyue. "A mixture-energy-consistent six-equation two-phase numerical model for fluids with interfaces, cavitation and evaporation waves." *Journal of Computational Physics* 259 (2014): 331-357.

[15] Saurel, Richard, Fabien Petitpas, and Rémi Abgrall. "Modelling phase transition in metastable liquids: application to cavitating and flashing flows." *Journal of Fluid Mechanics* 607 (2008): 313-350.

[16] Zhang, Ju. "A simple and effective five-equation two-phase numerical model for liquid-vapor phase transition in cavitating flows." *International Journal of Multiphase Flow* 132 (2020): 103417.